Electrochemical oxidation of thallium (I) in groundwater by employing single-chamber microbial fuel cells as renewable power sources

Tian, Caixing; Zhang, Baogang; Borthwick, Alistair G.L.; Li, Yunlong; Liu, Wen

Published in:
International Journal of Hydrogen Energy

DOI:
10.1016/j.ijhydene.2017.10.026

Publication date:
2017

Electrochemical oxidation of thallium (I) in groundwater by employing single-chamber microbial fuel cells as renewable power sources

Caixing Tian[a], Baogang Zhang[a*], Alistair G.L. Borthwick[b], Yunlong Li[a], Wen Liu[c*]

[a] *School of Water Resources and Environment, China University of Geosciences Beijing, Key Laboratory of Groundwater Circulation and Evolution (China University of Geosciences Beijing), Ministry of Education, Beijing 100083, China*

[b] *School of Engineering, The University of Edinburgh, The King's Buildings, Edinburgh EH9 3JL, UK*

[c] *College of Environmental Sciences and Engineering, Peking University, The Key Laboratory of Water and Sediment Sciences, Ministry of Education, Beijing 100871, China*

[*]Corresponding author. Tel.: +86 10 8232 2281; Fax: +86 10 8232 1081. E-mail: zbgcugb@gmail.com, baogangzhang@cugb.edu.cn (B. Zhang)

Tel.: +86 10 6275 4292; Fax: +86 10 6275 4292. E-mail: liuwensee@pku.edu.cn (W. Liu)

Abstract

An aerated electrochemical reactor (AER) employing single-chamber microbial fuel cells (MFCs) as renewable power sources is proposed for Tl(I) removal in groundwater. 80.5% of Tl(I) is oxidized to Tl(III) after 4 h electrolysis with initial Tl(I) concentration of 5 mg L^{-1}, pH of 2.0, and applied voltage of 600 mV. Comparison experiments indicate that Tl(I) oxidation is mainly attributed to indirect electrochemical oxidation by *in situ* generated H_2O_2. Carbon felt performs best as anode material, while lower initial Tl(I) concentration, pH and higher applied voltage promote Tl(I) removal efficiencies. Subsequent coagulation/precipitation realizes nearly complete removal of total Tl from groundwater. Besides as renewable power source, MFC can also remove residual total Tl in the exhausted solution from AER efficiently. Analysis of the generated precipitate further confirms that Tl(III) is the main oxidation state of Tl. This work proves that the AER driven by low bioelectricity from MFC is a cost-effective process with *in situ* produced advanced oxidants to remove T1(I) from groundwater satisfactorily.

Keywords: Microbial fuel cells; Thallium (I); Electrochemical oxidation; Bioelectricity generation

1. Introduction

Thallium (Tl) is a trace metal classified as a priority pollutant by the US Environmental Protection Agency (EPA) based on two concerns. First, thallium has higher toxicity than other heavy metals including Hg, Cd, and Pb. Second, there is increasing risk of Tl leaking into the environment because of accidents given the extensive use of Tl in industry as well as through active geological processes [1-4]. Thus the contaminant level of Tl in drinking water set by EPA is as low as 2 μg L^{-1} [5]. Typically, Tl exists in two oxidation states: Tl(I) and Tl(III) [6]. Tl(I) is usually considered to be the dominant species as it is more soluble, mobile and bioavailable than Tl(III) which tends to precipitate and form complexes with greater stability [7-9]. Tl(I) concentrations up to 1100 μg L^{-1} have been detected in deep groundwater within Tl-mineralized areas, and it is difficult to achieve natural oxidation in the hypoxic environment of groundwater [10]. It is imperative that effective and economic methods be developed to remove Tl from contaminated groundwater, especially Tl(I). Physical-chemical processes are often employed because of the acute toxicity of Tl to microbes [11, 12]. Of these processes, adsorption has received considerable attention, but also has drawbacks due to the complicated preparation process required, difficulties in adsorbent regeneration, and blockage problems [1, 13]. Alternatively, electrochemical oxidation has been recognized as a promising process for removals of highly toxic substances from water, including various bio-refractory organic compounds and heavy metals [14, 15]. Oxidation of Tl(I) to readily precipitated Tl(III) is regarded as a more efficient process for control of Tl pollution [16]. However,

higher levels of applied voltage (almost up to 10 V) or current (almost up to 12 A/dm^2) are often necessary for traditional electrochemical processes [17, 18]. This is the major factor restricting practical application of electrochemical technology.

Microbial fuel cells (MFCs) can convert chemical energy into electricity by utilizing bacteria as catalysts to oxidize organic and inorganic matter [19, 20], and have become a topic of intense research interest in the context of wastewater treatment as an innovative technology with potentially major environmental benefits [21-23]. Water contaminated by heavy metals with high redox potentials have been successfully treated in the cathode chamber of a MFC through abiotic reduction, including cadmium [24], chromium [25], vanadium [26], silver [27], and copper [28], along with bioelectricity generation. Moreover, redox sensitive metals as vanadium and arsenic can also be removed from aqueous solution in the anode chamber of MFCs [29, 30], with the similarity of nutrients removals [31, 32]. Additionally, the bioelectricity produced by MFCs has been used directly to remove heavy metals such as As(III) at reduced cost based on MFC-zerovalent iron hybrid process, relying on the *in situ* H_2O_2 production in the cathode of MFCs [33]. Besides environmental applications, MFCs have been explored to be used as renewable power supplies intensively nowadays for health and monitoring purpose [34, 35]. Furthermore, electrosynthesis of active substances driven by MFCs has been successfully employed for metals and organics removals from water [33, 36, 37]. While few studies have been carried out on the physical and chemical processes involved in electrochemical oxidation of Tl(I) based on MFC technology and characteristics of Tl, along with

removals of the oxidation products from aqueous solution.

A novel aerated electrochemical reactor (AER) driven by bioelectricity from MFCs is proposed for effective Tl(I) oxidation. The performance of MFCs in terms of power supply and Tl(I) oxidation behavior in the AER are evaluated. Influencing factors affecting the performance as well as mechanisms of Tl(I) oxidation and subsequent total Tl removal are intensively investigated. The results confirm that the MFC powered electrochemical system provides an efficient, cost-effective means of controlling Tl pollution in groundwater.

2. Materials and methods

2.1 System buildings

Experiments were conducted in an electrochemical system consisting of an AER mainly responsible for Tl(I) oxidation and an MFC acting as the power supply. A single-chamber air-cathode MFC comprising a cubic chamber of effective volume equal to 125 mL (5 × 5 × 5 cm) was built, following Zhang et al. [38]. Carbon fiber felt (4 × 4 × 1 cm) served as the anode, whereas the cathode was fabricated from 16 cm^2 plain carbon paper with 0.5 mg cm^{-2} of Pt catalyst coating on the water-facing side. Anode and cathode were connected through a 1000 Ω external resistor by copper wire with a layer of insulating plastic to close the circuit during the start-up period. Connections between copper wire and electrodes were sealed with insulation glue to prevent their exposure to air or water. The MFC was inoculated with 25 mL anaerobic sludge obtained from a well-functioning anaerobic reactor. Nutrient solution

containing (per liter) NH_4Cl (0.13 g); KCl (0.13 g); $NaH_2PO_4 \cdot H_2O$ (4.97 g); $Na_2HPO_4 \cdot H_2O$ (2.75 g); vitamins (1.25 mL); trace minerals (12.5 mL) and 750 mg L^{-1} glucose served as anolyte. The pH of this growth medium maintained around 7 with the function of added phosphate buffer solution.

The AER comprised a glass beaker with 200 mL working volume. The anode was constructed from carbon felt, and the cathode from graphite plate. Both were rectangular (geometric dimensions of 2.5 × 4 cm) and positioned vertically as well as parallel to each other with an inter-electrode gap of 1 cm. They were connected to the MFC by copper wire. A variable resister was also introduced into the circuit to obtain the desired voltage across the AER. A small aeration device was used to supply dissolved oxygen to the cathode at a flow rate of 2.5 L min^{-1}. Two similar glass beakers were also employed to conduct the comparison experiments involving solely aeration or solely electrolysis.

2.2 Experimental procedures

Successful start-up of the MFC was achieved by refreshing the electrolyte every day with the fixed external resistance of 1000 Ω, after which its power output performance was monitored. Prior to electrolysis, the electrodes of the AER were immersed in the target solutions for 4 h to exclude the adsorption influence. Then electrochemical oxidation of Tl(I) for an initial Tl(I) concentration of 5 mg L^{-1} and pH of 2.0 was evaluated by measuring the production of Tl(III) as the generated Tl(III) was soluble under this condition. The applied voltage was fixed at 600 mV and the pH

was adjusted by adding 0.1 M HCl. Active substances and oxidation efficiency were monitored synchronously to study the oxidation mechanisms, and the results were compared with those from control experiments. Experiments were also conducted with addition of $FeSO_4$-EDTA (0.1 mM) as H_2O_2 scavenger to confirm its functions during Tl(I) oxidation as Fe(II) could be firstly oxidized to Fe(III) by H_2O_2 if it existed in the solution to realize the removals of H_2O_2 [39, 40]. Then influencing factors as anode materials (carbon felt, carbon cloth, graphite plate), initial Tl(I) concentration (1 mg L^{-1}, 5 mg L^{-1},10 mg L^{-1},15 mg L^{-1}), initial pH (1.5, 2.0, 2.5, 3.0), applied voltage (200 mV, 400 mV, 600 mV, 700 mV) were examined separately. Subsequent coagulation/precipitation experiments were also performed to remove total Tl from the exhausted electrolyte [1, 41], i.e. direct precipitation by adjusting the pH to 9 by 1 M NaOH, addition of ferric chloride (2.5 g $FeCl_3$•$6H_2O$) or polymeric ferric sulfate (PFS) with magnetic stirring and pH of 9. Then the solution was filtered through a suction filter with 0.22 μm membrane. Tl(III) and total Tl were examined in the filtrate and the intercepted precipitate was analyzed by X-ray photoelectron spectroscopy (XPS). All experiments were conducted in triplicate at ambient temperature (22 ± 2 ºC) and mean values of experimental data were reported.

2.3 Analytical methods

The concentration of Tl(III) was monitored by a UV-vis spectrophotometer (DR 5000, HACH, USA) at 505 nm [42]. Flame atomic absorption spectrophotometry (ASC-990, Persee, China) was employed to determine the concentration of total Tl. The generation of hydrogen peroxide was analyzed by the spectrophotometer at 350

nm, after the sample was mixed with 0.1 M potassium iodide and 0.01M ammonium heptamolybdate tetrahydrate [43, 44]. pH was measured by a pH-201meter (Hanna, Italy). XPS analysis was performed to determine the elemental composition and oxidation sate of Tl using Al *K*α X-ray at 15 kV and 15 mA (XSAM-800, Kratos, UK). The standard C 1s peak (Binding energy, E_b = 284.80 eV) was used to eliminate the static charge effects. A data acquisition system (PMD1208LS, Measurement Computing Corp., Norton, MA, USA) was employed to monitor voltage outputs at 5 min intervals. Polarization curves were plotted to evaluate the performance of the MFCs and obtain the maximum power density by varying external resistances from 5000 Ω to 10 Ω using a resistor box. Current density and power density were normalized by the single-side projected cathode surface area.

3. Results and Discussion

3.1 Evaluation of power outputs of the MFC

Successful start-up of the MFC was confirmed using an external resistance of 1000 Ω, until reproducible cycles of voltage production were obtained (Fig. 1a). Electrochemically active bacteria classified as Bacteroidetes and Proteobacteria were accumulated, as indicated by our previous study [45]. Then the AER was connected directly to the MFC and the voltage outputs of the MFC monitored were 300 - 750 mV in the presence of fresh anolyte. Satisfactory repeatability was exhibited for consecutive multiple cycles (Fig. 1a), similar results have also been obtained previously in tests of bio-electro-reactors for refractory organics removal [36]. Our

results indicated that the present MFC could be utilized as a renewable power source supplying bioelectricity for electrolysis experiments.

With fresh anolyte, the polarization curve was also obtained for a closed circuit, and a maximum power density of 518.5 mW m^{-2} was obtained (Fig. 1b), comparable with results from single-chamber MFC systems fed with simple organic substrate, such as acetate or glucose [46]. Similar power output levels have also been observed in an MFC-zero-valent iron hybrid process for arsenite removal [33]. Moreover, the power density produced herein was much higher than achieved in two-chamber bio-electro systems (about 300 mW m^{-2}) [47, 48], implying that higher oxidation efficiencies of pollutants could be achieved with higher power outputs from a single chamber MFC.

3.2 Tl(I) oxidation behavior and mechanisms

Once the voltage across the AER was settled at 600 mV by adjusting the variable resistor, obvious Tl(I) removal was observed from solution containing Tl(I) at initial concentration of 5 mg L^{-1} and initial pH of 2.0 in the AER with carbon felt anode (Fig. 2). An oxidation efficiency of nearly 80.5% for Tl(I) was achieved within 4 h operation, exhibiting the significant advantage of the present technology over previous Tl(I) removal processes, which represented a major improvement on previous studies for Tl(I) removals through bioaccumulation with removal efficiency of only 58.8% in 30 days [14, 49]. Moreover, Tl(I) was gradually oxidized to Tl(III) with its concentration increased accordingly during the operation (Fig. 2). Though

Tl(III) is more toxic than Tl(I), the former has weak mobility and so readily precipitates before being removed from water; this is an improvement on adsorption which is limited by the requirement of continual regeneration of the adsorbent [50]. The present technology offered considerable promise for prospective application to thallium removal from groundwater.

Comparison experiments were conducted in order to investigate the key mechanisms (Fig. 2). Oxidation of Tl(I) was rarely detected with aeration without applied voltage, suggesting that Tl(I) could hardly be oxidized by oxygen as previously indicated [51]. Furthermore, direct and indirect electrochemical effects are key aspects of the electrolysis system. Only about 10.0% of Tl(I) was transformed to Tl(III) in 4 h operating cycle with applied voltage of 600 mV, replacing aeration with magnetic stirring, illustrating that direct electrolysis contributed little as the relatively lower applied voltage of 600 mV, compared to traditional electrochemical process [52]. In view of the nearly 80.5% Tl(I) removed in the proposed AER, indirect electrochemical oxidation was confirmed as the main effect. Similar conclusions were also drawn in our previous study for methyl orange decolorization [53].

Active substances generated in the AER were also monitored to confirm the indirect electrochemical effect. The concentration of hydrogen peroxide increased continuously within 4 h (Fig. 2), in agreement with results from our previous bio-electro decolorization system [54]. Hydrogen peroxide was produced due to the reduction of oxygen in the AER, which was responsible for Tl(I) oxidation. With the addition of scavenger to remove hydrogen peroxide, Tl(I) removals were significantly

suppressed in the AER (Fig. 2), further confirming the key roles of the generated hydrogen peroxide during Tl(I) oxidation. Unlike electro-Fenton reactors, hydroxyl radicals were rarely generated due to the omission of catalysis by Fe^{2+} [37]. Moreover, typical costs of this electrochemically produced hydrogen peroxide between 0.1 and 0.3 \$ kg^{-1} were much lower than those for hydrogen peroxide production by the traditional anthraquinone process (between 1 and 2 \$ kg^{-1}) [54], exhibiting the cost-effectiveness of the present technology. Additionally, although reported yields of hydrogen peroxide in the cathode of dual chamber MFCs were higher than those obtained in our study [55], their performances were affected by high internal resistance caused by separator [37]. Though there were also two reactors required as the dual chamber MFCs, this modified two-reactor electrochemical system using the power produced by a single-chamber MFC to drive the *in situ* hydrogen peroxide production provided an alternative based on MFCs with the reduction of costs and elimination of the effect of membrane by omitting the membrane [36, 37], as over 60% of the material cost of the MFCs are due to the proton exchange membrane [56]. Even proton exchange membrane could be replaced by relatively inexpensive ion-exchange membranes as separators, they still occupied a large part of the cost of MFCs [57]. The lower hydrogen peroxide production could be contributed to the increase of internal resistance of MFCs due to the distances between anode and cathode [58]. Further efforts could be made to improve the yields of H_2O_2 from electrode materials, reactor configurations and operational optimization.

Figure 3 depicted the electron transfer processes in the proposed system. In the

MFC anode, glucose was oxidized to CO_2 and H_2O by bacteria, with the production of electrons and protons (Eq. (1)). Electrons then flowed through copper wires to the cathode of the AER, where oxygen was reduced to H_2O_2 (Eq. (2)). In the anode of the AER, Tl(I) was oxidized to Tl(III) by the *in situ* generated H_2O_2 (Eq. (3)) as well as the direct electrochemical oxidation process (Eq. (4)). Then electrons transferred to the cathode of the MFC where oxygen was reduced to H_2O (Eq. (5)).

$$C_6H_{12}O_6 + 6H_2O \rightarrow 6CO_2 + 24H^+ + 24e^- \quad (1)$$

$$O_2 + 2H^+ + 2e^- \rightarrow H_2O_2 \quad (2)$$

$$Tl^+ + H_2O_2 + 4Cl^- + 2H^+ \rightarrow TlCl_4^- + 2H_2O \quad (3)$$

$$Tl^+ + 4Cl^- \rightarrow TlCl_4^- + 2e^- \quad (4)$$

$$O_2 + 4H^+ + 4e^- \rightarrow 2H_2O \quad (5)$$

After 4 h operation, the pH increased from 2.0 to 2.13. The generated Tl(III) could easily form soluble complexes ($TlCl_4^-$) with chloride ion because Tl(III) was strongly binded to unidentate ligands (Cl^-) under this condition to prevent Tl(III) from becoming hydrolyzed, which was conducive to promoting the oxidation of Tl(I) and subsequent coagulation/precipitation reactions because of the long chain and large molecular weight of the complexes [50]. Thus the importance of HCl in achieving total Tl removals was highlighted. Concentrations of total Tl were rarely changed (Fig. 2), thus influencing factors and subsequent treatment were necessarily studied to achieve prospective applications of the proposed system and total Tl removal from groundwater.

3.3 Investigations of influencing factors

Anode materials had great influence on AER performance, thus different carbon materials which were commonly used in electrochemical process were evaluated. Relatively lower Tl(I) removals were observed when both carbon cloth and graphite plate were employed as anodes in the AER with applied voltage of 600 mV, initial concentration of 5 mg L^{-1} and initial pH of 2.0, while its oxidation efficiency increased to 80.5% after 4 h operation with carbon felt anode (Fig. 4a). The superior performance of carbon felt could be attributed to its relatively larger specific surface area, which could facilitate the transfer of electrons and provide abundant reaction sites for the Tl(I) oxidation. Similar results were also obtained in our previous study [36].

Figure 4b showed that higher initial concentration of Tl(I) resulted in lower Tl(I) oxidation efficiency in the AER with carbon felt anode, applied voltage of 600 mV and initial pH of 2.0. A rapid and complete oxidation of Tl(I) was observed within 4 h with initial Tl(I) concentration of 1 mg L^{-1}. Nevertheless, with the initial Tl(I) concentration up to 5 mg L^{-1} and 10 mg L^{-1}, the oxidation efficiency of Tl(I) decreased to 80.5% and 64.1%, respectively. This might be ascribed to the limited generation of active substances due to lower applied voltage from MFC.

Tl(I) oxidation efficiency increased with the decrease of initial pH in the AER with carbon felt anode, applied voltage of 600 mV and initial concentration of 5 mg L^{-1} (Fig. 4c). A significant improvement on Tl(I) oxidation efficiency from 10.2% to

nearly 100% was noticed when the initial pH decreased from 3.0 to 1.5. pH was the key factor for electrochemical production of hydrogen peroxide while the *in situ* generated hydrogen peroxide was mainly responsible for the oxidation of Tl(I) to Tl(III). Moreover, the abundant added Cl^- under lower pH also facilitated Tl(I) removal as chlorion-related oxidants could be produced for oxidizing Tl(I) and the generated Tl(III) could form stable complexes with Cl^- [59].

Figure 4d illustrated that the oxidation efficiency of Tl(I) increased with the increase of applied voltage in the AER with carbon felt anode, initial concentration of 5 mg L^{-1} and initial pH of 2.0. Obviously, a significant improvement of Tl(I) oxidation efficiency was realized with applied voltage increasing from 200 mV to 600 mV. Especially, with the applied voltage up to 700 mV, a rapid Tl(I) oxidation with efficiency of nearly 100% was achieved within 4 h. The applied voltage also affected the production of hydrogen peroxide and higher voltage resulted in its larger yield, which could promote the oxidation of Tl(I).

3.4 Subsequent treatment for total Tl removal

All the three processing methods employed in the subsequent coagulation/precipitation experiments for the exhausted solution from the AER could realize the removal of total Tl (Fig. 5). Nearly all the total Tl could be removed with addition of ferric chloride through the bridge formation and catching-sweeping mechanism in flocculating process. The removal efficiency of total Tl with PFS was slightly lower than with ferric chloride while direct adjusting the pH of exhausted

electrolyte to 9 only realized about 25% of total Tl removal. Meanwhile, direct treatment of raw Tl(I) solution by adding the same amount of ferric chloride was also performed, and total Tl was rarely removed due to the strong mobility of Tl(I) [40]. After this process, most added Fe^{3+} precipitated with thallium, preventing secondary pollution for groundwater. The foregoing results demonstrated that the proposed process i.e. oxidation in the AER and subsequent coagulation/precipitation with ferric chloride was capable of controlling Tl pollution effectively. It could be combined with pump-and-treat methods for practical remediation of Tl-contaminated groundwater in future. Furthermore, MFC was an emerging technique for environmental contaminations removals and toxic heavy metals with redox sensitive characteristics had been biochemically handled [22]. Thus we also introduced the effluent of AER after adjusting its pH to 7 and adding 750 mg L^{-1} glucose to the anode chamber of MFC. As the oxidation products of Tl(I) are insoluble under neutral conditions, changes of total Tl were employed to reflect Tl(I) removals. After 7 d operation, 67.9% of residual total Tl was removed in the MFC (Fig. 5). Tl(I) and glucose acted as electron donors and Tl(I) was bio-electrochemically oxidized through co-metabolisms pathway, with anodic electrode as electron acceptor and simultaneous precipitation of oxidation products. Similar phenomenon had also been found for As(III) removals in the anode of MFCs [40]. Under this situation, slight declines of maximum power density from 518.5 mW m^{-2} to 431.6 mW m^{-2} were observed due to the high toxicity of Tl to microbes [4], but the voltage outputs above 600 mV could also be maintained when the AER was connected to this MFC fed with the

Tl-containing medium, implying that the MFC could also function well as power sources under this situation with removing Tl(I) simultaneously. When 5 mg L^{-1} Tl(I) was directly added into the MFC, hardly any Tl(I) were removed, probably as microbes could not survive with such high concentration Tl(I) [6]. This provided another alternative for subsequently handling the exhausted solution from the AER and distinguishes MFC from any other fuel cells or batteries as power sources. It should be noted that the proposed system in Fig. 3 played key roles to remove Tl(I) significantly when treating water with high concentration of Tl(I), which was of particular importance to application of MFC as subsequent treatment unit. Otherwise Tl(I) under high concentration could suppress and even poison microbes in the anode of MFCs [7]. The treatment of Tl(I) contaminated groundwater in AER and MFC in sequence could be further investigated afterwards.

XPS analysis was carried out on the generated precipitates during the ferric chloride and PFS treatment, respectively (Fig. 6a). The spectrum had a peak corresponding to Tl 4f and measured banding energy located at 118.2 eV, which could be ascribed to Tl(III) [60]. The presence of O 1s and Fe 2p with the respective peaks located at approximately 531.1eV and 711.0 eV corresponded to nucleophilic oxygen (O^{2-}) and Fe^{3+}, thus the oxides were inferred to be Fe_2O_3, due to slow decomposition of the weak base ($Fe(OH)_3$) [61]. The lack of a peak corresponding to Tl(I) at 119.05 eV in the high resolution of Tl 4f in Fig. 6b indicated that scarcely any Tl(I) existed in the precipitate [62]. This meant that Tl(I) was oxidized almost completely to Tl(III) in the AER and the latter deposited subsequently on the surface of $Fe(OH)_3$ or Fe_2O_3,

provided by ferric chloride or PFS, resulting in effective removals of total Tl from aqueous solution.

4. Conclusions

With MFC as renewable power supply, 80.5% of Tl(I) was removed in the AER under conditions within 4 h. The majority of Tl(I) oxidation attributed to indirect electrochemical oxidation by *in situ* generated H_2O_2 and Tl(III) was the main oxidation product. Principles of influencing factors were also revealed. Subsequent coagulation/precipitation realized the nearly complete removal of total Tl. Residual total Tl in the exhausted solution from AER could also be removed efficiently in the MFC employed as renewable power supply. XPS spectrum analysis revealed that Tl(III) was the primary oxidation state of Tl. This work provides an alternative for Tl(I) removal from contaminated groundwater via an electrochemical system powered by bioelectricity from MFC.

Acknowledgements

This research work was supported by Beijing Nova Program (No. Z171100001117082).

References

[1] Birungi ZS, Chirwa EMN. The adsorption potential and recovery of thallium using green micro-algae from eutrophic water sources. J Hazard Mater 2015;299:67-77.

[2] Nielsen SG, Rehkämper M, Brandon AD, Norman MD, Turner S, O'Reilly SY.

Thallium isotopes in Iceland and Azores lavas -Implications for the role of altered crust and mantle geochemistry. Earth Planet Sci Lett 2007;264:332-45.

[3] Rajesh N, Subramanian MS. A study of the extraction behavior of thallium with tribenzylamine as the extractant. J Hazard Mater 2006;135:74-7.

[4] Liu J, Wang J, Chen Y, Lippold H, Xiao T, Li H, et al. Geochemical transfer and preliminary health risk assessment of thallium in a riverine system in the Pearl River Basin. South China J Geochem Explor 2017;176:64-75.

[5] Memon SQ, Memon N, Solangi AR, Memon JR. Sawdust: A green and economical sorbent for thallium removal. Chem Eng J 2008;140:235-40.

[6] Rickwood CJ, King M, Huntsman-Mapila P. Assessing the fate and toxicity of Thallium I and Thallium III to three aquatic organisms. Ecotoxicol Environ Saf 2015;115:300-8.

[7] John Peter AL, Viraraghavan T. Thallium: a review of public health and environmental concerns. Environ Int 2005;31:493-501.

[8] Sangvanich T, Sukwarotwat V, Wiacek RJ, Grudzien RM, Fryxell GE, Addleman RS, et al. Selective capture of cesium and thallium from natural waters and simulated wastes with copper ferrocyanide functionalized mesoporous silica. J Hazard Mater 2010;182:225-31.

[9] Arbab-Zavar MH, Chamsaz M, Zohuri G, Darroudi A. Synthesis and characterization of nano-pore thallium (III) ion-imprinted polymer as a new sorbent for separation and preconcentration of thallium. J Hazard Mater 2011;185:38-43.

[10] Xiao T, Boyle D, Guha J, Rouleau A, Hong Y, Zheng B. Groundwater-related thallium transfer processes and their impacts on the ecosystem: southwest Guizhou Province, China. Appl Geochem 2003;18:675-91.

[11] John Peter AL, Viraraghavan T. Removal of thallium from aqueous solutions by modified Aspergillus niger biomass. Bioresour Technol 2008;99:618-25.

[12] Şenol ZM, Ulusoy U. Thallium adsorption onto polyacryamide-aluminosilicate composites: A Tl isotope tracer study. Chem Eng J 2010;162:97-105.

[13] Mueller RF. Microbially mediated thallium immobilization in bench scale systems. Mine Water Environ 2001;20:17-29.

[14] Ling Y, Hu J, Qian Z, Zhu L, Chen X. Continuous treatment of biologically treated textile effluent using a multi-cell electrochemical reactor. Chem Eng J 2016;286:571-7.

[15] Shen R, Liu Z, He Y, Zhang Y, Lu J, Zhu Z, et al. Microbial electrolysis cell to treat hydrothermal liquefied wastewater from cornstalk and recover hydrogen: Degradation of organic compounds and characterization of microbial community. Int J Hydrogen Energ 2016;41:4132-42.

[16] Tong M, Yuan S, Wang Z, Luo M, Wang Y. Electrochemically induced oxidative removal of As(III) from groundwater in a dual-anode sand column. J Hazard Mater 2016;305:41-50.

[17] Beauchesne I, Drogui P, Seyhi B, Mercier G, Blais JF. Simultaneous electrochemical leaching and electrodeposition of heavy metals in a single-cell process for wastewater sludge treatment. J Environ Eng 2014;140:481-6.

[18] Figueroa G, Valenzuela JL, Parga JR, Vazquez V, Valenzuela A. Recovery of gold and silver and removal of copper, zinc and lead ions in pregnant and barren cyanide solutions. Mater Sci Appl 2015;6:171-82.

[19] Zhang B, Zhang J, Liu Y, Hao C, Tian C, Feng C, et al. Identification of removal principles and involved bacteria in microbial fuel cells for sulfide removal and electricity generation. Int J Hydrogen Energy 2013;38:14348-55.

[20] Liu L, Tsyganova O, Lee DJ, Chang JS, Wang A, Ren N. Double-chamber microbial fuel cells started up under room and low temperatures. Int J Hydrogen Energy 2013;35:15574-9.

[21] Santoro C, Ieropoulos I, Greenman J, Cristiani P, Vadas T, Mackay A, et al. Power generation and contaminant removal in single chamber microbial fuel cells (SCMFCs) treating human urine. Int J Hydrogen Energy 2013;38:11543-51.

[22] Winfield J, Chambers LD, Rossiter J. Towards disposable microbial fuel cells: Natural rubber glove membranes. Int J Hydrogen Energy 2014;39:21803-10.

[23] Sonawane J, Adeloju S, Ghosh P. Landfill leachate: A promising substrate for microbial fuel cells. Int J Hydrogen Energ 2017;42: 23794-8.

[24] Chen Y, Shen J, Huang L, Pan Y, Quan X. Enhanced Cd(II) removal with simultaneous hydrogen production in biocathode microbial electrolysis cells in the presence of acetate or $NaHCO_3$. Int J Hydrogen Energ 2016;44:13368-79.

[25] Huang L, Chai X, Cheng S, Chen G. Evaluation of carbon-based materials in tubular biocathode microbial fuel cells in terms of hexavalent chromium

reduction and electricity generation. Chem Eng J 2011;166:652-61.

[26] Zhang B, Feng C, Ni J, Zhang J, Huang W. Simultaneous reduction of vanadium (V) and chromium (VI) with enhanced energy recovery based on microbial fuel cell technology. J Power Sources 2012;204:34-9.

[27] Tao H, Gao Z, Ding H, Xu N, Wu W. Recovery of silver from silver(I)-containing solutions in bioelectrochemical reactors. Bioresour Technol 2012;111:92-7.

[28] Gajda I, Stinchcombe A, Greenman J, Melhuish C, Ieropoulos I. Microbial fuel cell - A novel self-powered wastewater electrolyser for electrocoagulation of heavy metals. Int J Hydrogen Energ 2017;42:1813-9.

[29] Hao L, Zhang B, Cheng M, Feng C. Effects of various organic carbon sources on simultaneous V(V) reduction and bioelectricity generation in single chamber microbial fuel cells. Bioresour Technol 2016;201:105-10.

[30] Li Y, Zhang B, Cheng M, Li Y, Hao L, Guo H. Spontaneous arsenic (III) oxidation with bioelectricity generation in single-chamber microbial fuel cells. J Hazard Mater 2016;306:8-12.

[31] Liu H, Zhang B, Liu Y, Wang Z, Hao L. Continuous bioelectricity generation with simultaneous sulfide and organics removals in an anaerobic baffled stacking microbial fuel cell. Int J Hydrogen Energy 2015;40:8128-36.

[32] Huang Y, Huang Y, Liao Q, Fu Q, Xia A, Zhu X. Improving phosphorus removal efficiency and Chlorella vulgaris growth in high-phosphate MFC wastewater by frequent addition of small amounts of nitrate. Int J Hydrogen

Energy 2017; In press.

[33] Xue A, Shen Z, Zhao B, Zhao H. Arsenite removal from aqueous solution by a microbial fuel cell-zerovalent iron hybrid process. J Hazard Mater 2013;261:621-7.

[34] Song T, Wang D, Wang H, Li X, Liang Y, Xie J. Cobalt oxide/nanocarbon hybrid materials as alternative cathode catalystfor oxygen reduction in microbial fuel cell. Int J HydrogenEnergy 2015;40:3868-74.

[35] Wang A, Liu W, Cheng S, Xing D, Zhou J, Logan BE. Source of methane and methods to control its formation in single chamber microbial electrolysis cells. Int J Hydrogen Energy 2009;34:3653-8.

[36] Wang Z, Zhang B, Borthwick AGL, Feng C, Ni J. Utilization of single-chamber microbial fuel cells as renewable power sources for electrochemical degradation of nitrogen-containing organic compounds. Chem Eng J 2015;280:99-105.

[37] Zhu X, Logan BE. Using single-chamber microbial fuel cells as renewable power sources of electro-Fenton reactors for organic pollutant treatment. J Hazard Mater 2013;252:198-203.

[38] Zhang J, Zhang B, Tian C, Ye Z, Liu Y, Lei Z, et al. Simultaneous sulfide removal and electricity generation with corn stover biomass as co-substrate in microbial fuel cells. Bioresour Technol 2013;138:198-203.

[39] Chen Y, Lu A, Li Y, Zhang L, Yip H, Zhao H, et al. Naturally occurring sphalerite as a novel cost-effective photocatalyst for bacterial disinfection under visible light. Environ Sci Technol 2011;45:5689-95.

[40] Li Y, Zhang B, Borthwick AGL, Long Y. Efficient electrochemical oxidation of thallium (I) in groundwater using boron-doped diamond anode. Electrochim Acta 2016;222:1137-43.

[41] Guo X, Wei Z, Wu Q, Li C, Qian T, Zheng W. Effect of soil washing with only chelators or combining with ferric chloride on soil heavy metal removal and phytoavailability: Field experiments. Chemosphere 2016;147:412-9.

[42] Revanasiddappa HD, Kiran Kumar TN. A simple and rapid spectrophotometric determination of thallium(III) with trifluoperazine hydrochloride. Anal Sci 2002;18:1131-5.

[43] Jin Y, Dai Z, Liu F, Kim H, Tong M, Hou Y. Bactericidal mechanisms of Ag_2O/TNBs under both dark and light conditions. Water Res 2013;47:1837-47.

[44] Liu W, Ni J, Yin X. Synergy of photocatalysis and adsorption for simultaneous removal of Cr(VI) and Cr(III) with TiO_2 and titanate nanotubes. Water Res 2014;53:12-25.

[45] Zhang B, Tian C, Liu Y, Hao L, Liu Y, Feng C, et al. Simultaneous microbial and electrochemical reductions of vanadium (V) with bioelectricity generation in microbial fuel cells. Bioresour Technol 2015;179:91-7.

[46] Wang X, Feng Y, Wang H, Qu Y, Yu Y, Ren N, et al. Bioaugmentation for electricity generation from corn stover biomass using microbial fuel cells. Environ Sci Technol 2009;43:6088-93.

[47] Feng C, Li F, Mai H, Li X. Bio-electro-Fenton process driven by microbial fuel cell for wastewater treatment. Environ Sci Technol 2010;44:1875-80.

[48] Zhuang L, Zhou S, Yuan Y, Liu M, Wang Y. A novel bioelectro-Fenton system for coupling anodic COD removal with cathodic dye degradation. Chem Eng J 2010;163:160-3.

[49] Urík M, Kramarová Z, Ševc J, Čerňanský S, Kališ M, Medve J, et al. Biosorption and bioaccumulation of thallium (I) and its effect on growth of Neosartorya fischeri strain. Pol J Environ Stud 2010;19:457-60.

[50] Chung NH, Nishimoto J, Kato O, Tabata M. Selective extraction of thallium (III) in the presence of gallium (III), indium (III), bismuth (III) and antimony (III) by salting-out of an aqueous mixture of 2-propanol. Anal Chim Acta 2003;477:243-9.

[51] Casiot C, Egal M, Bruneel O, Verma N, Parmentier M, Elbaz-Poulichet F. Predominance of aqueous Tl(I) species in the river system downstream from the abandoned carnoules mine (Southern France). Environ Sci Technol 2011;45:2056-64.

[52] Zhang P, Tong M, Yuan S, Liao P. Transformation and removal of arsenic in groundwater by sequential anodic oxidation and electrocoagulation. J Contam Hydrol 2014;164:299-307.

[53] Zhang B, Wang Z, Zhou X, Shi C, Guo H, Feng C. Electrochemical decolorization of methyl orange powered by bioelectricity from single-chamber microbial fuel cells. Bioresour Technol 2015;181:360-2.

[54] Barazesh JM, Hennebel T, Jasper JT, Sedlak DL. Modular advanced oxidation process enabled by cathodic hydrogen peroxide production. Environ Sci

Technol 2015;49:7391-9.

[55] Young MN, Chowdhury N, Garver E, Evans PJ, Popat SC, Rittmann BE, et al. Understanding the impact of operational conditions on performance of microbial peroxide producing cells. J Power Sources 2017;356:448-58.

[56] Ge Z, He Z. Long-term performance of a 200 liter modularized microbial fuel cell system treating municipal wastewater: treatment, energy, and cost. Environ Sci Water Res Technol 2016;2:274-81.

[57] Flores GH, Varaldo HMP, Feria OS. Comparison of alternative membranes to replace high cost Nafion ones in microbial fuel cells. Int J Hydrogen Energy 2016;41:23354-62.

[58] Asghar A, Raman AAA, Wan MAWD. Advanced oxidation processes for in-situ production of hydrogen peroxide/hydroxyl radical for textile wastewater treatment: a review. J Clean Prod 2015;87:826-38.

[59] Zhang L, Huang T, Zhang M, Guo X, Yuan Z. Studies on the capability and behavior of adsorption of thallium on nano-Al_2O_3. J Hazard Mater 2008;157:352-7.

[60] Wan S, Ma M, Lv L, Qian L, Xu S, Xue Y, et al. Selective capture of thallium(I) ion from aqueous solutions by amorphous hydrous manganese dioxide. Chem Eng J 2014;239:200-6.

[61] Liu W, Zhang P, Borthwick AGL, Chen H, Ni J. Adsorption mechanisms of thallium(I) and thallium(III) by titanate nanotubes: ion-exchange and co-precipitation. J Colloid Interface Sci 2014;423:67-75.

[62] Casella IG, Spera R. Electrochemical deposition of nickel and nickel-thallium composite oxides films from EDTA alkaline solutions. J Electroanal Chem 2005;578:55-62.

Figure Captions

Fig. 1. (a) Voltage outputs and (b) polarization curves of the employed MFC.

Fig. 2. Time history of Tl(I) removal, total Tl change and hydrogen peroxide generation in the AER as well as the control results.

Fig. 3. Proposed pathways of Tl(I) oxidation and bioelectricity generation in the proposed system.

Fig. 4. Influencing factors studies for Tl(I) oxidation in the AER. (a) anode materials; (b) initial Tl(I) concentration; (c) initial pH; and (d) applied voltage.

Fig. 5. Performance of total Tl removal in the subsequent coagulation/precipitation experiments as well as in MFC.

Fig. 6. (a) XPS survey spectra and (b) high resolution of Tl 4f for the precipitate from subsequent coagulation/precipitation with ferric chloride and PFS.

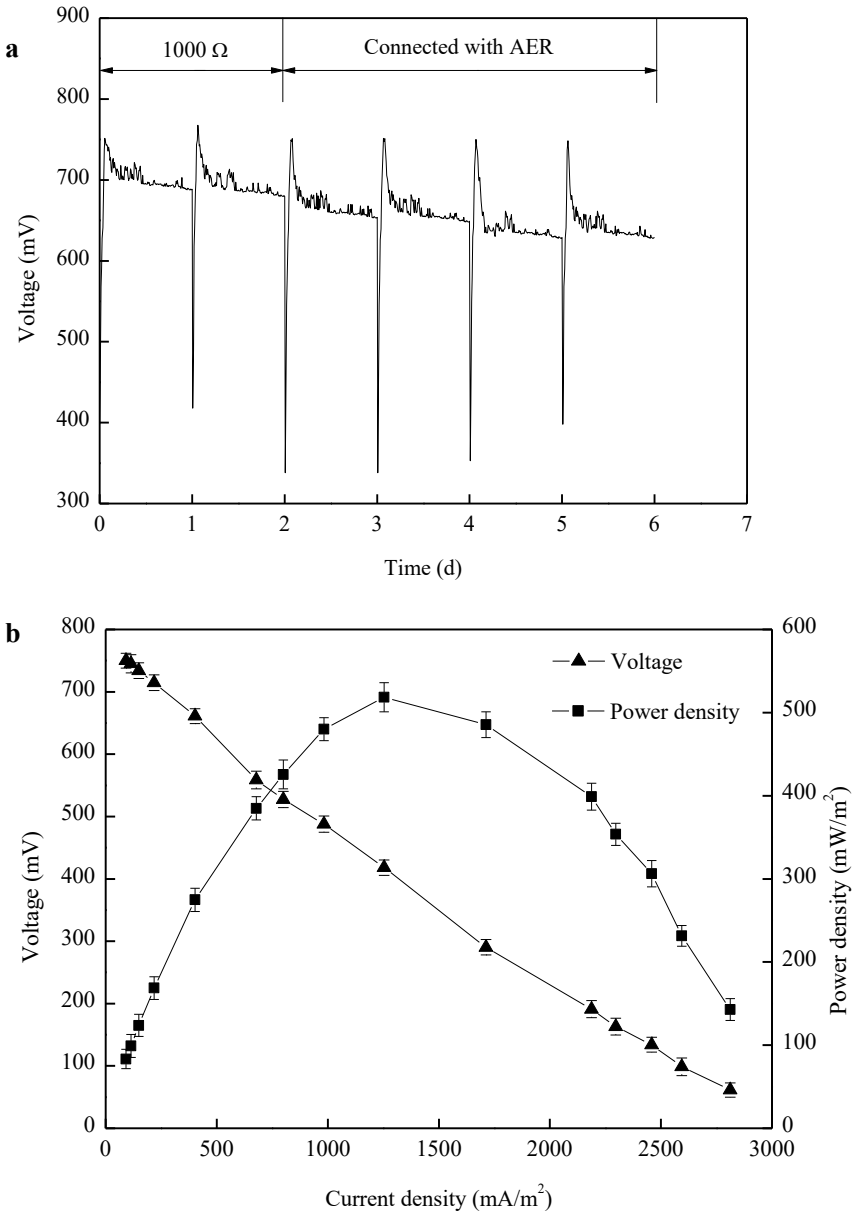
a
1000 Ω
Connected with AER
Voltage (mV)
Time (d)
b
Voltage
Power density
Voltage (mV)
Power density (mW/m^2)
Current density (mA/m^2)

Figure 1

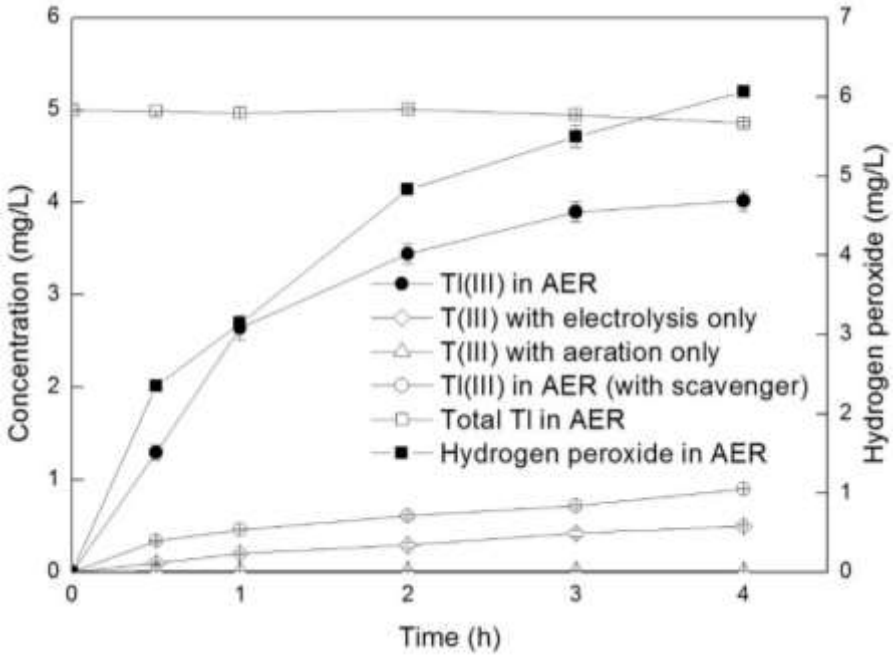
Concentration (mg/L)
Hydrogen peroxide (mg/L)
Time (h)
Tl(III) in AER
T(III) with electrolysis only
T(III) with aeration only
Tl(III) in AER (with scavenger)
Total Tl in AER
Hydrogen peroxide in AER
0
1
2
3
4
5
6
7

Figure 2

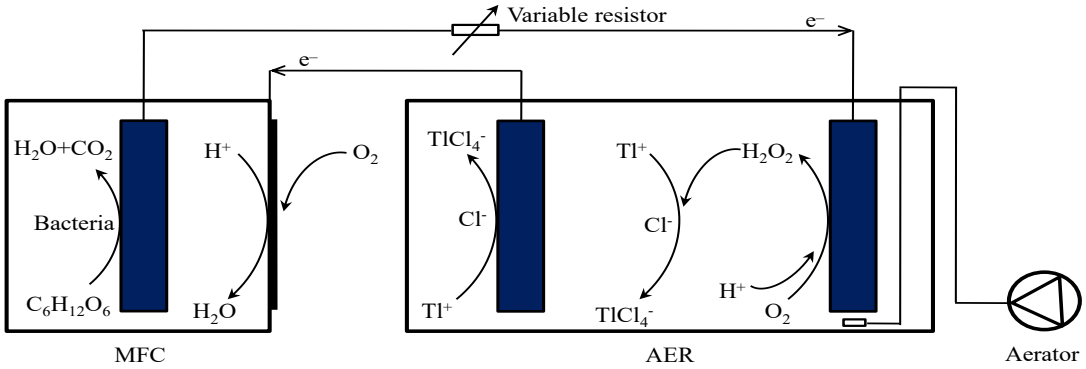
Variable resistor
e⁻
e⁻
H2O+CO2
Bacteria
C6H12O6
H+
H2O
O2
TlCl4-
Cl-
Tl+
Tl+
Cl-
TlCl4-
H2O2
H+
O2
MFC
AER
Aerator

Figure 3

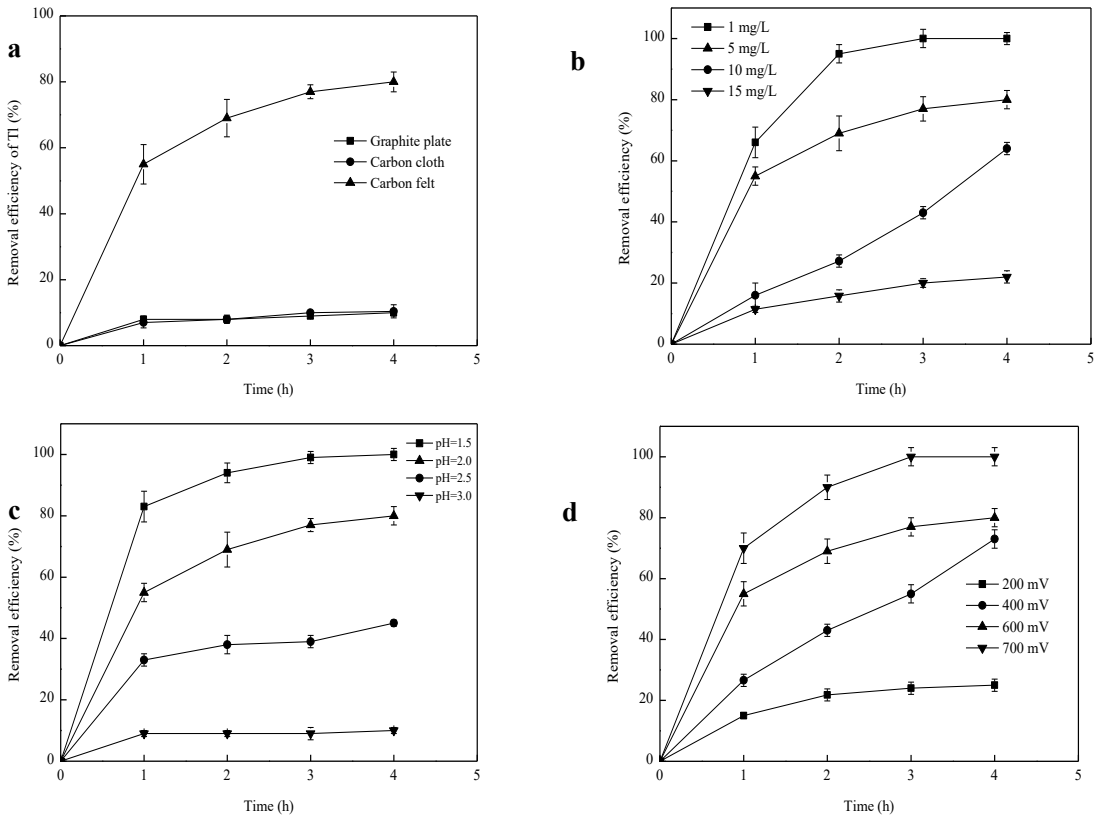
a
Removal efficiency of Tl (%)
Time (h)
Graphite plate
Carbon cloth
Carbon felt
b
Removal efficiency (%)
Time (h)
1 mg/L
5 mg/L
10 mg/L
15 mg/L
c
Removal efficiency (%)
Time (h)
pH=1.5
pH=2.0
pH=2.5
pH=3.0
d
Removal efficiency (%)
Time (h)
200 mV
400 mV
600 mV
700 mV

Figure 4

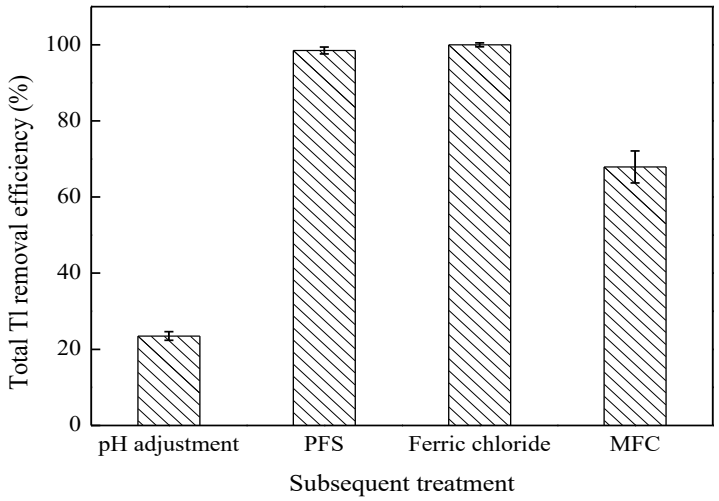
Total Tl removal efficiency (%)
0
20
40
60
80
100
pH adjustment
PFS
Ferric chloride
MFC
Subsequent treatment

Figure 5

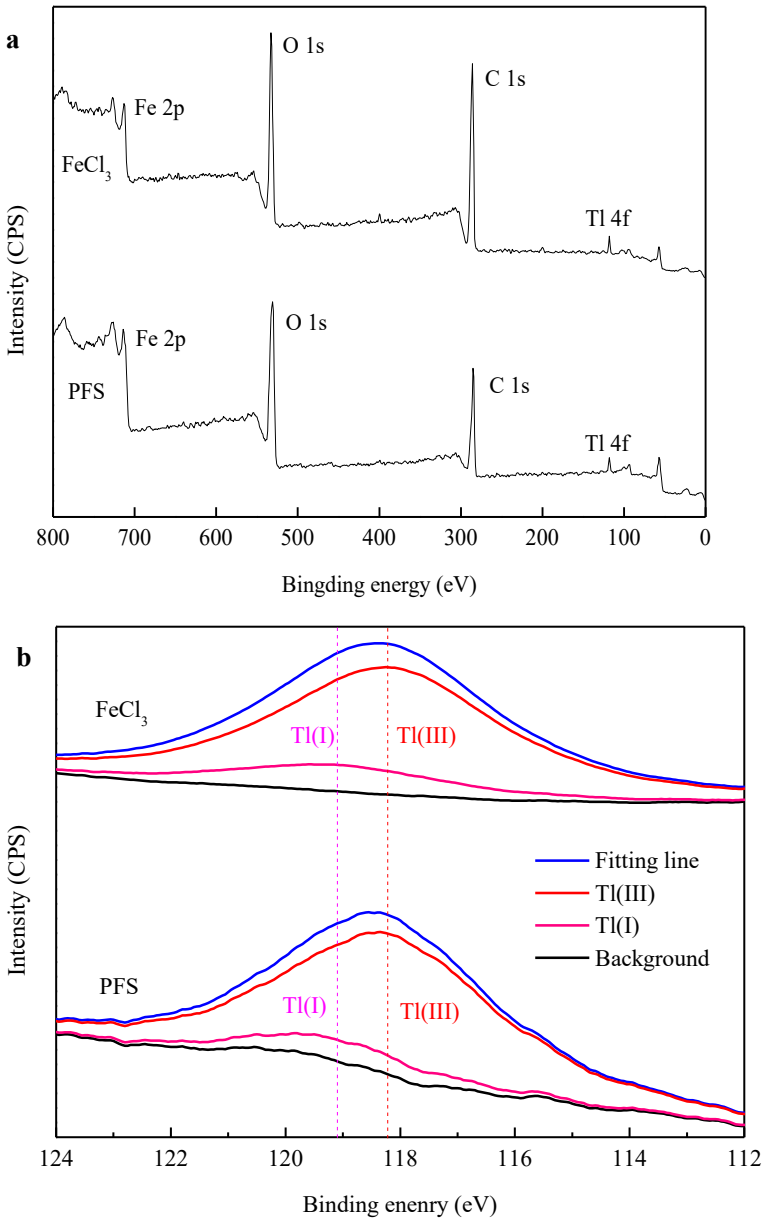
a
O 1s
C 1s
Fe 2p
FeCl3
Tl 4f
O 1s
Fe 2p
PFS
C 1s
Tl 4f
Intensity (CPS)
800
700
600
500
400
300
200
100
0
Bingding energy (eV)
b
FeCl3
Tl(I)
Tl(III)
Fitting line
Tl(III)
Tl(I)
Background
PFS
Tl(I)
Tl(III)
Intensity (CPS)
124
122
120
118
116
114
112
Binding enenry (eV)

Figure 6